INTERNATIONAL JOURNAL OF CLIMATOLOGY
Int. J. Climatol. **27**: 903–909 (2007)
Published online 14 November 2006 in Wiley InterScience
(www.interscience.wiley.com) DOI: 10.1002/joc.1450

RMetS
ROYAL METEOROLOGICAL SOCIETY

Drought reconstruction for north central China from tree rings: the value of the Palmer drought severity index

Jinbao Li,[a,b] Fahu Chen,[a]* Edward R. Cook,[b] Xiaohua Gou[a] and Yongxiang Zhang[a]
[a] *CAEP, MOE Key Laboratory of West China's Environmental System, Lanzhou University, Lanzhou 730000, China*
[b] *Tree-Ring Laboratory, Lamont-Doherty Earth Observatory, Columbia University, NY 10964, USA*

Abstract:

We present a drought reconstruction for north central China based on a tree ring-width chronology developed from two sites of the Chinese pine (*Pinus tabulaeformis*) in the northern Helan Mountains. The drought reconstruction, spanning 1788–1999 A.D., was developed by calibrating tree-ring data with the Palmer drought severity index (PDSI), an index that describes the regional moisture condition properly. The reconstruction was verified with independent data, and accounts for 45.7% of the actual PDSI variance during their common period (1941–1999). The full reconstruction indicates that the regional drought variability was relatively stable during the nineteenth century, but became more variable and persistent during the twentieth century. The drought epoch in the late 1920s was the most severe one in our reconstruction. In contrast to a wetting trend in the western area of northwest China, a clear drying trend has occurred in north central China since mid-1930s. The multitaper method (MTM) spectral analysis indicates the existence of some decadal (~11.4 year) and interannual (9.1, 6.8, 4.0, 2.7 and 2.1–2.0 year) cycles, which may potentially be the fingerprints of some proposed climate change forcings. Copyright © 2006 Royal Meteorological Society

KEY WORDS dendroclimatology; drought; PDSI; north central China

Received 31 January 2006; Revised 6 September 2006; Accepted 24 September 2006

INTRODUCTION

The drought variation in north central China has strong effects on regional social and agricultural activities. In 2001, the worst drought since 1990 hit this and surrounding areas, leaving million hectares of land parched and millions of people and livestock short of drinking water (People's Daily, 31 May, 2001). The occurrence of this drought may be part of a larger-scale drying trend in central, north and northeast China since the 1950s (Wang and Zhou, 2005; Zou *et al*., 2005). Furthermore, recent studies indicate that the increasing intensity of global warming may contribute to the development of more frequent and persistent droughts (Cook *et al*., 2004; Dai *et al*., 2004; Trenberth *et al*., 2004). Therefore, it is of great importance to investigate the characteristics of drought variability and its potential forcing mechanisms for north central China, an area where moisture availability is critical to the survival of human populations and the ecosystems.

Direct instrumental records offer valuable insights on current drought variability. However, a complete understanding of drought cannot be achieved without a long-term perspective, particularly when considering defining its current status and identifying possible trends and periodicities. To this end, the value of tree rings for reconstructing past droughts has been demonstrated by numerous studies (e.g., Fritts, 1976; Stahle *et al*., 1985; Graumlich, 1993; Cook *et al*., 1999; Pederson *et al*., 2001).

The Palmer drought severity index (PDSI; Palmer, 1965) is a widely used meteorological drought index across the United States and for much of the globe (Briffa *et al*., 1994; Cook *et al*., 1999; Heim, 2002; Lloyd-Hughes and Saunders, 2002; Ntale and Gan, 2003; Cook *et al*., 2004; Dai *et al*., 2004; Zou *et al*., 2005; D'Arrigo *et al*., 2006; van der Schrier *et al*., 2006). It was developed by Palmer (1965) as a means to measure moisture conditions by incorporating antecedent precipitation, soil moisture demand and supply into a primitive hydrological accounting system. Positive PDSI values indicate wetter conditions, while negative values indicate dryer conditions. The PDSI is most suitable for describing soil moisture and streamflow changes. The primary advantage of the PDSI is its ability to detect and quantify the severity of dry and wet conditions across space and time (Alley, 1984; Keyantash and Dracup, 2002). For China, using the PDSI as a drought indicator is particularly valuable because both precipitation and potential evapotranspiration need to be considered in order to describe moisture conditions (Wu *et al*., 2006).

Currently, the use of PDSI for drought reconstructions from tree rings over China is under exploration. Our

* Correspondence to: Fahu Chen, CAEP, MOE Key Laboratory of West China's Environmental System, Lanzhou University, Lanzhou 730000, China. E-mail: fhchen@lzu.edu.cn

recent study demonstrated its feasibility for drought reconstruction in the western area of northwest China, and revealed a long-term trend toward an intensified moisture regime during the twentieth century (Li *et al*., 2006a). Here we describe another case study to show its great potentials for drought reconstructions over north central China. Our purposes in this study are to (1) examine the relationship between tree growth and soil moisture availability, which are indicated by the ring-width chronology and the PDSI respectively, and (2) reconstruct and investigate long-term drought variability for the study area.

MATERIALS AND DATA

The Helan Mountains are located in north central China where the arid northwest meets the Loess Plateau (Figure 1). They extend over 200 km from south to north, but only 15–60 km from east to west. The elevation of the Helan Mountains is normally at 2000–3000 m a.s.l. Located along the northwest margin of the East Asian Summer Monsoon, the Helan Mountains act as a barrier to the penetration of monsoon rainfall into northwest China as well as to the intrusion of deserts into north and central China. Not surprisingly, the vegetation growing there is quite sensitive to monsoon-related climate variations.

Our tree-ring data were collected from two sites in the northern Helan Mountains (BSI and SYK; Figure 1; Table I). The soil at both sites was thin and rocky. The dominant tree species in both forests was Chinese pine (*Pinus tabulaeformis*), which was typically found growing at an elevation zone of 1900–2350 m a.s.l. (Li and Hu, 2002). Some juniper (*Juniperus rigida*), spruce (*Picea crassifolia*) and birch (*Populus davidiana*) trees were also found in these forests.

Increment cores were extracted from the Chinese pines at both sites. After air drying, mounting and sanding in the laboratory, all the samples were carefully crossdated by visual comparison, and each ring-width was subsequently measured to 0.001 mm precision. The COFECHA program (Holmes, 1983) was further employed to check the quality of visual crossdating. These methods ensure exact dating for each annual growth ring.

As shown in Figure 2, the mean ring-width series of the two sites agreed well with each other, despite the long distance between the two sites and their different slope orientations. Therefore, all the raw measurements were standardized to develop one ring-width chronology

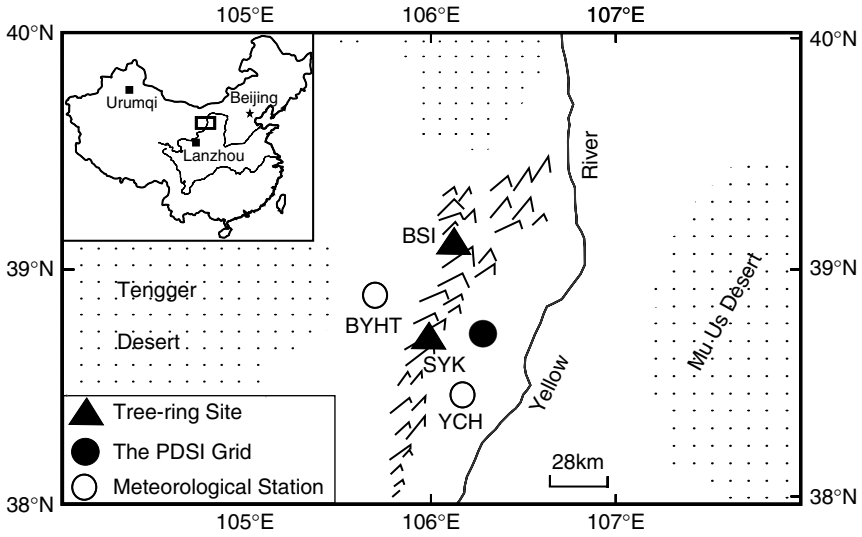

Figure 1. Map showing the two tree-ring sampling sites, two meteorological stations and the nearest PDSI grid point developed by *Dai et al.* (2004)

Table I. Statistics of the two tree-ring sites, two meteorological stations and the nearest PDSI grid point developed by *Dai et al.* (2004).

Data type	Site code	Location (latitude; longitude)	Elevation (m)	Number (core/tree)	Time span (A.D.)
Tree-ring	BSI	39°05′N, 106°05′E	2000–2350	41/25	1738–1999
	SYK	38°43′N, 105°59′E	1900–2400	66/40	1717–1999
Meteorological data	BYHT	38°50′N, 105°40′E	1561	–	1953–1999
	YCH	38°29′N, 106°13′E	1111	–	1951–1999
PDSI	–	38°45′N, 106°15′E	–	–	1941–2003

DOI: 10.1002/joc

to indicate the regional climate signal. The chronology was developed with the ARSTAN program (Cook, 1985) by removing biological growth trends while preserving variations that were likely related to climate. Most series were conservatively detrended by fitted negative exponential curves (39 series) or linear regression curves of any slope (43 series). A cubic spline with a 50% frequency-response cutoff equal to 67% of the series length was used in a few cases (25 series) when the significant growth reversal from the 1920s to the 1930s resulted in poor curve fits based on conservative detrending. To reduce the potential influence due to the changing sample depth, the variance of the chronology was also stabilized using the method described in Osborn *et al.* (1997). Finally, the subsample signal strength (SSS; Wigley *et al.*, 1984) with a threshold value of 0.85 was used to evaluate the most reliable time span of the chronology. On the basis of these techniques, we consider our ring-width chronology to be valid for dendroclimatic study. The final chronology extends from 1788 A.D. to 1999 A.D., is composed of data from 107 cores of 65 trees and has a mean segment length of 171 years.

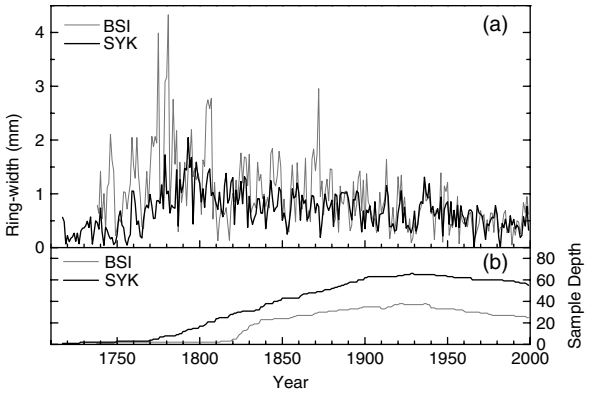

Figure 2. (a) The mean ring-width measurements of samples at the site of BSI and SYK and (b) their corresponding sample depths

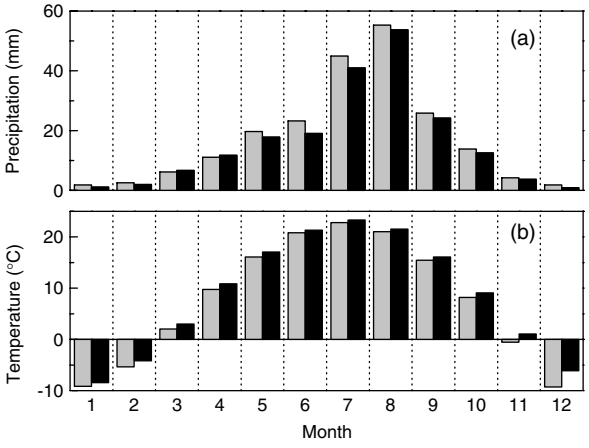

Figure 3. (a) Monthly total precipitation and (b) monthly mean temperature records at the meteorological station of BYHT (light bars) and YCH (solid bars) during 1953–1999

The climate data used in this study include local meteorological records (i.e. temperature and precipitation) as well as the monthly PDSI data developed by Dai *et al.* (2004) (Table I). The local instrumental data covering the period 1953–1999 were obtained from two nearby meteorological stations (BYHT and YCH; Figure 1). Another nearby high-elevation station had only 30-year records (1961–1990) and was therefore excluded from our study due to statistical considerations. The PDSI dataset developed by Dai *et al.* (2004) is available on a $2.5^\circ \times 2.5^\circ$ grid. The grid point nearest to our sampling sites was used in this study (Figure 1).

CORRELATION ANALYSES OF TREE RINGS WITH CLIMATE DATA

As shown in Figure 3, the patterns of monthly temperature and precipitation at BYHT and YCH are almost identical to each other, indicating large-scale climate uniformity in the study area. However, the precipitation at BHYT is marginally higher than that at YCH, while the opposite is true for temperature. This pattern is at least partially due to the discrepancy in their site elevations (Table I). At any rate, we have used the average values of both sites to indicate the regional mean climate condition during the instrumental period.

Climate-growth responses were analyzed for the common period when both meteorological records and tree-ring data were available (i.e. 1953–1999). The analyses were performed over a dendroclimatic year (Fritts, 1976) from last October to current September. As shown in Figure 4(a), the precipitation in May and June of the current growing season is positively correlated with tree growth. In contrast, the temperature during the current growing season is negatively correlated with tree growth, especially in March and August. Clearly, both temperature and precipitation play important roles in modulating tree growth in the study area, as both affect soil moisture availability. The potential evapotranspiration demand, an important factor affecting soil water balance, is directly modulated by temperature and has been shown to relate highly to tree growth (LeBlanc and Terrell, 2001). Wu *et al.* (2006) also showed that potential evapotranspiration in our study area has a different trend in different seasons. Considering all the facts mentioned so far, we look for a drought index that takes all these factors into consideration – the PDSI.

Correlations of tree rings with monthly PDSI data over their common period 1941–1999 were further analyzed. As the PDSI is a direct measure of soil moisture availability, we analyzed their correlations for the current growth season (i.e. March–October) when correlations with precipitation were the highest. As shown in Figure 4(b), most of the correlations are significant at the 95% confidence level, except those in September and October. Peak correlation occurred in June ($r = 0.67$), followed by the correlations in May ($r = 0.58$) and March ($r = 0.55$). As

DOI: 10.1002/joc

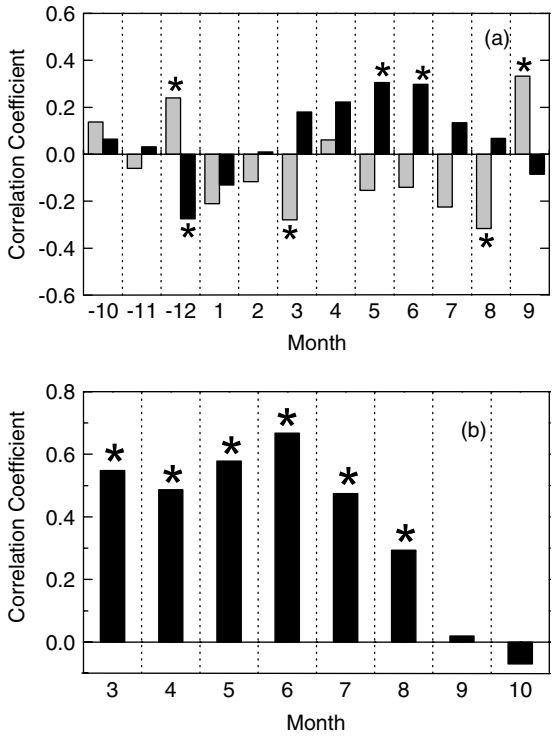

Figure 4. Correlations of tree rings with (a) monthly precipitation (solid bars) and temperature records (light bars) during 1953–1999, and with (b) monthly PDSI data during 1941–1999. The asterisks indicate the correlations at or over 95% confidence levels

indicated by the overall correlation pattern between tree rings and the PDSI, the soil moisture availability in the early and middle growth season plays a critical role in tree growth, while late growth season moisture availability is less important.

Seasonally averaged PDSI may be more representative of moisture conditions during the growing season than just one single month (Cook *et al*., 1999). Therefore, we tested different seasonal combinations of PDSI for drought reconstruction. The highest correlation between tree rings and the seasonalized PDSI was found in March–July ($r = 0.68$; $p < 0.0001$), which agrees well with the monthly correlations in Figure 4(b). We therefore used March–July as the drought reconstruction season.

CALIBRATION AND VERIFICATION OF THE RECONSTRUCTION MODEL

A simple linear regression model (Cook and Kairiukstis, 1990) was used to reconstruct the drought history of the northern Helan Mountains of north central China. During the common period of tree rings and the PDSI data (1941–1999), the reconstruction accounted for 45.7% of the actual PDSI variance (Table II). As shown in Figure 5, despite the general fact that trees tend to underestimate extreme climate conditions, especially those on the wetter side of the model, our reconstruction successfully captured both high- and low-frequency variations of local moisture availability.

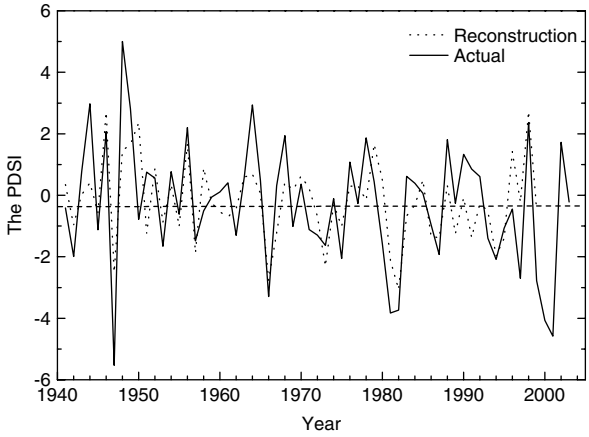

Figure 5. Actual (solid line) and estimated (dotted line) March–July PDSI during their common period 1941–1999. Note that the actual PDSI data during 2000–2003 are also shown here to facilitate our understanding on the recent moisture trend

Split-sample calibration-verification tests (Meko and Graybill, 1995) were further employed to evaluate the statistical fidelity of our reconstruction model. The resulting statistics are shown in Table II. The values of the two most rigorous tests of model validation, the reduction of error (RE) and the coefficient of efficiency (CE), are both positive, which indicates significant skill in the tree-ring estimates. The results of the sign test, which describes how well the predicted value tracks the direction of actual data, exceed the 95% confidence level. These test results demonstrate the validity of our regression model. On the basis of this model, the drought history in the study area has been reconstructed for the period 1788–1999 A.D. (Figure 6).

DROUGHT RECONSTRUCTION AND DISCUSSION

Our reconstruction quantitatively extends the drought history in the Helan Mountains back to 1788 A.D., providing a longer background to evaluate local moisture variability (Figure 6). The mean value of our PDSI reconstruction is −0.17, which is within the scale of

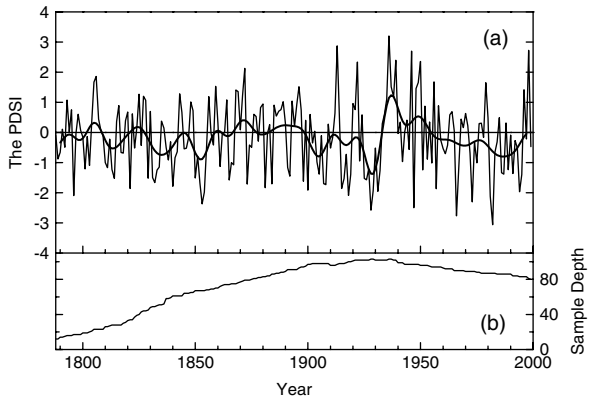

Figure 6. (a) Reconstruction of March–July PDSI (solid line) for 1788–1999 and its 5-year running average (bold line), and (b) the corresponding sample depth

DOI: 10.1002/joc

Table II. Statistics of calibration and verification test results.

	Calibration (1941–1970)	Verification (1971–1999)	Calibration (1971–1999)	Verification (1941–1970)	Full calibration (1941–1999)
r	0.696	0.624	0.624	0.696	0.676
r^2	0.484	0.389	0.389	0.484	0.457
RE	–	0.450	–	0.492	–
CE	–	0.317	–	0.414	–
Sign test	22/8[b]	21/8[a]	20/9[a]	21/9[a]	–

[a] Significance at $p < 0.05$.
[b] Significance at $p < 0.01$.

the defined normal moisture status (PDSI $= 0.0 \pm 0.5$) (Palmer, 1965). However, the reconstructed PDSI values fall mainly within ± 3, which is only about half of the PDSI amplitude of the actual data (± 6; Figure 5). We therefore rescaled the PDSI reconstruction to achieve values closer to those of the actual data over the calibration period. Doing so indicated that PDSI values of (≤ -1.0 or ≥ 1.0) represent severely dry or wet conditions and the values of (≤ -2.0 or ≥ 2.0) represent extremely dry or wet conditions. These adjusted cutoffs are used as the basis for our interpretations of the reconstruction to follow.

Our reconstruction indicates that moisture conditions in the study area were quite variable. Severely dry years accounted for 27.4% (58) of the years during the whole reconstruction, while the severely wet years accounted for 15.6% (33) of the years. This asymmetry in the frequency of severely dry and wet years may be partially due to the way in which trees may respond more fully to extremes that most strongly limit growth, in this case, soil moisture deficits. We also note that if the long-term mean of the reconstruction (-0.17) is adjusted upward to zero, this apparent asymmetry in the estimates reduces considerably. Doing so changes the frequency of severely dry years in the reconstruction from 27.4% (58 years) to 23.1% (49 years) and severely wet years from 15.6% (33 years) to 18.9% (40 years). Making this adjustment may be justified by the fact that PDSI as originally formulated by Palmer (1965) is known to produce somewhat bimodal distributions of PDSI, with the strongest mode falling either slightly below zero or slightly above zero (Wells and Goddard, 2004). Consequently, the apparent bias in our reconstruction may not be as serious as first indicated.

The extreme years of PDSI in the reconstruction are less affected by the asymmetry induced by the way the PDSI is calculated. The extremely dry and wet years (PDSI ≤ -2.0 or ≥ 2.0 by our definition here) accounted for 4.2% (9 years) and 3.8% (8 years), respectively. An adjustment for the nonzero mean does not appreciably change these frequencies, and most of the extremely dry or wet years occurred in the twentieth century.

The longer-lasting dry or wet events generally have much stronger effects on local social and agricultural activities. The droughts lasting over four years were found in 1831–1834, 1850–1854, 1915–1919 and 1925–1932. As indicated by our reconstruction, the drought epoch in 1925–1932 is the most severe and long-lasting drought in the study area since 1788 A.D. (Figure 6). This drought appears to have occurred over a large geographic area, as it has also been evidenced by many studies over the surrounding regions (Pederson *et al*., 2001; Liang *et al*., 2003; Liu *et al*., 2003). Meanwhile, the long-lasting wet spells are uncommon in our reconstruction. The wet spell in 1935–1939 is the only one that lasted over four years. The wet spell in 1946–1950 is almost comparable with the one in 1935–1939, but it was interrupted by an extreme drought in 1947.

With respect to long-term changes in the regional moisture variability, two stages can be identified in our reconstruction: a relatively stable nineteenth century and a highly unstable twentieth century (Figure 6). Regional moisture conditions during the nineteenth century were relatively stable, especially in the second half of the century (see the 5-year moving average in Figure 6). Similar reductions of low-frequency drought-related variations during the late nineteenth century were also found in the surrounding areas (Pederson *et al*., 2001; Li *et al*., 2006a), suggesting some common forcings may exist for large-scale drought variability over these areas.

The most noteworthy feature in our reconstruction occurred in the twentieth century. With a growing background of global warming, moisture conditions in the study area have become more persistent and unstable. The most severe drought epoch since 1788 A.D. occurred in the late-1920s, which was followed by the wettest period of the past 200 years in the mid-1930s. On the basis of the available meteorological records or PDSI data, many studies have evidenced a drying trend in central, north and northeast China since the 1950s (Wang and Zhou, 2005; Zou *et al*., 2005). Our reconstruction is in basic agreement with this assessment. As further evidenced by the actual PDSI data (Figure 5), this drying trend has basically persisted up to 2003 and may go further, even though it was interrupted by the extremely wet event in 1998 when most parts of central and northeast China were devastated by severe floods. This drying trend is in contrast to a wetting trend in the western area of northwest China, which has been attributed to the increased strength of the Asian Southwest Monsoon (Li *et al*., 2006b). The

DOI: 10.1002/joc

increase in the monsoon strength appears to be related to warming of sea surface temperatures over the northern Indian Ocean, which is considered to be part of the global warming trend. However, whether global warming caused the drying trend over north central China still needs further investigation.

The multitaper method (MTM) of spectral analysis (Mann and Lees, 1996) was further employed to examine the characteristics of local drought variability in the frequency domain. The analysis was performed over the full range of our reconstruction (i.e. 1788–1999 A.D.). As shown in Figure 7, a decadal broadband power (at 95% level) peaking at 11.4 years was identified for local drought variability. The waveform of the 11.4-year cycle, as extracted by the MTM method, accounts for 14.7% of the total variance during 1788–1999. This decadal cycle resembles other findings in surrounding areas and suggests the influence of solar forcing on the climate there (Pederson *et al*., 2001; Liu *et al*., 2003; 2006a).

Significant high-frequency peaks were found at 9.1-year (90%), 6.8-year (90%), 4.0-year (90%), 2.7-year (95%) and 2.1–2.0 year (99%). Most of these interannual cycles (i.e. 6.8, 4.0, 2.7 and 2.1–2.0 year) fall within the range of El Niño-Southern Oscillation (ENSO) variability (Allan *et al*., 1996), suggesting strong teleconnections between ENSO and the drought variability in north central China. This finding is consistent with early studies that showed ENSO has strong effects on the interannual variations of summer rainfall in northern China (Zhang *et al*., 1999; Feng and Hu, 2004). Meanwhile, these interannual cycles are also within the signal bands of the Arctic Oscillation (AO), whose high-frequency components were also considered to be tropically forced (Lin *et al*., 2002; Jevrejeva *et al*., 2003). The strong biennial (2.0–2.1 year) cycle also resembles the variability of tropical biennial oscillation (TBO; Meehl, 1987). Overall, these high-frequency cycles suggest the moisture variability in the study area may have strong associations with large-scale ocean–atmosphere–land circulation systems.

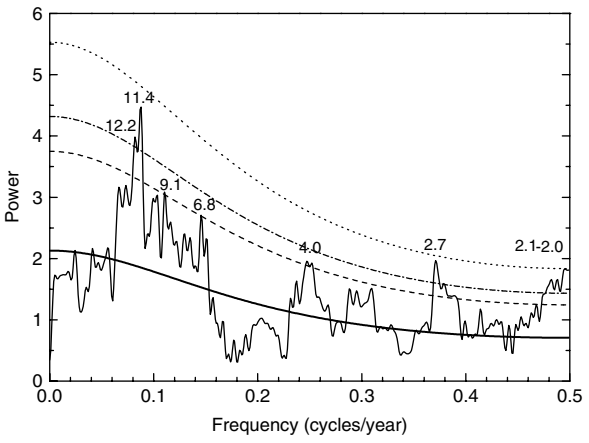

Figure 7. MTM spectral density of the drought reconstruction. The bold line indicates the null hypothesis; the dash, dash-dot and dotted lines indicate the 90, 95 and 99% significance level respectively

CONCLUSIONS

The results of our study indicate the feasibility of combining tree rings and the PDSI for drought reconstructions in north central China. Using this method, further large-scale drought reconstruction can be conducted for this area. Preliminary results of our reconstruction for the northern Helan Mountains have revealed regional moisture variations during 1788–1999. As indicated in our study, regional moisture variability has increased and become more persistent during the twentieth century, and a clear drying trend has occurred since the mid-1930s. Spectral analysis results indicate that regional moisture variability over north central China is possibly influenced by multiple large-scale climate forcings; among them some might be changing due to global warming.

Admittedly, our preliminary drought reconstruction is only based on samples from two sites and covers only the last two centuries. Therefore, it is of critical importance to further develop large-scale and long-term drought reconstructions over this and surrounding areas. These efforts will enable us to better understand problems such as the recent trend toward dryer conditions in north central China, the climate forcings responsible for the observed changes in regional moisture variability and the strategies for future water resources management.

ACKNOWLEDGEMENTS

The authors thank Neil Pederson and one anonymous reviewer for their critical comments. We are also thankful to Gordon Jacoby, Rosanne D'Arrigo, Kevin L. Griffin and Paul J. Krusic. This research was supported by the Program of Introducing Talents of Discipline to Universities (B06026), Innovation Team Project (No.40421101), and NSFC Project (No.40201049 and No.40671191). This is a LDEO contribution 6982.

REFERENCES

Allan RJ, Lindesay JA, Parker DE. 1996. *El Niño Southern Oscillation and Climatic Variability*. CSIRO Publishing: Australia.

Alley WM. 1984. Palmer drought severity index: limitations and assumptions. *Journal of Climate and Applied Meteorology* **23**: 1100–1109.

Briffa KR, Jones PD, Hulme M. 1994. Summer moisture variability across Europe, 1892–1991: an analysis based on the Palmer drought severity index. *International Journal of Climatology* **14**: 475–506.

Cook ER. 1985. A time-series analysis approach to tree-ring standardization, PhD dissertation, The University of Arizona Press, Tucson.

Cook ER, Kairiukstis LA. 1990. *Methods of Dendrochronology*. Kluwer Academic Press: Netherlands.

Cook ER, Meko DM, Stahle DW, Cleaveland MK. 1999. Drought reconstructions for the continental United States. *Journal of Climate* **12**: 1145–1162.

Cook ER, Woodhouse CA, Eakin CM, Meko DM, Stahle DW. 2004. Long-term aridity changes in the western United States. *Science* **306**: 1015–1018.

Dai AG, Trenberth KE, Qian T. 2004. A global dataset of Palmer Drought Severity Index for 1870–2002: relationship with soil moisture and effects of surface warming. *Journal of Hydrometeorology* **5**: 1117–1130.

D'Arrigo R, Wilson R, Palmer J, Krusic P, Curtis A, Sakulich J, Bijaksana S, Zulaikah S, Ngkoimani LO. 2006. Monsoon drought

DOI: 10.1002/joc

over Java, Indonesia, during the past two centuries. *Geophysical Research Letters* **33**: L04709, Doi:10.1029/2005GL025465.
Feng S, Hu Q. 2004. Variations in the teleconnection of ENSO and summer rainfall in northern China: a role of the Indian summer monsoon. *Journal of Climate* **17**: 4871–4881.
Fritts HC. 1976. *Tree Rings and Climate*. Academic Press: London.
Graumlich LJ. 1993. A 1000-year record of temperature and precipitation in the Sierra Nevada. *Quaternary Research* **39**: 249–255.
Heim RR Jr. 2002. A review of twentieth-century drought indices used in the United States. *Bulletin of the American Meteorological Society* **83**: 1149–1165.
Holmes RL. 1983. Computer-assisted quality control in tree-ring dating and measurement. *Tree-ring Bulletin* **43**: 69–95.
Jevrejeva S, Moore JC, Grinsted A. 2003. Influence of the Arctic Oscillation and El Niño-Southern Oscillation (ENSO) on ice conditions in the Baltic Sea: the wavelet approach. *Journal of Geophysical Research* **108**(D21): 4677, Doi: 10.1029/2003JD003417.
Keyantash J, Dracup JA. 2002. The quantification of drought: an evaluation of drought indices. *Bulletin of the American Meteorological Society* **83**: 1167–1180.
LeBlanc D, Terrell M. 2001. Dendroclimatic analyses using Thornthwaite-Mather-type evapotranspiration models: a bridge between dendroecology and forest simulation models. *Tree-ring Research* **57**: 55–66.
Li T, Hu T. 2002. The research on the biological diversity and its values in Helan natural reserve in Ningxia Province. *Journal of Agriculture and Forestry Science and technology* **4**: 9–10.
Li JB, Gou XH, Cook ER, Chen FH. 2006a. Tree-ring based drought reconstruction for the central Tien Shan area in northwest China. *Geophysical Research Letters* **33**: L07715, Doi:10.1029/2006GL025803.
Li JB, Cook ER, Chen FH, Gou XH, D'Arrigo R. 2006b. Past moisture variability in Northwest China and its relationship to the Asian Southwest monsoon. *Climate Dynamics* (submitted).
Liang EY, Shao XM, Kong ZC, Lin JX. 2003. The extreme drought in the 1920s and its effect on tree growth deduced from tree ring analysis: a case study in North China. *Annals of Forest Science* **60**: 145–152.
Lin H, Derome J, Greatbath RJ, Peterson KA, Lu J. 2002. Tropical links of the Arctic Oscillation. *Geophysical Research Letters* **29**: 1943–1946, DOI: 10.1029/2002GL015822.
Liu Y, Cai QF, Park WK, An ZS, Ma LM. 2003. Tree-ring precipitation records from Baiyinaobao, Inner Mongolia since A.D. 1838. *Chinese Science Bulletin* **48**: 1140–1145.
Lloyd-Hughes B, Saunders MA. 2002. A drought climatology for Europe. *International Journal of Climatology* **22**: 1571–1592.
Mann ME, Lees J. 1996. Robust estimation of background noise and signal detection in climatic time series. *Climatic Change* **33**: 409–445.
Meehl GA. 1987. The annual cycle and interannual variability in the tropical Pacific and Indian Ocean region. *Monthly Weather Review* **115**: 27–50.
Meko DM, Graybill DA. 1995. Tree-ring reconstruction of Upper Gila River discharge. *Water Resources Bulletin* **31**: 605–616.
Ntale HK, Gan TY. 2003. Drought indices and their application to East Africa. *International Journal of Climatology* **23**: 1335–1357.
Osborn TJ, Briffa KR, Jones PD. 1997. Adjusting variance for sample-size in tree-ring chronologies and other regional mean time series. *Dendrochronologia* **15**: 89–99.
Palmer WC. 1965. *Meteorological Drought. Weather Bureau Res. Paper 45*. U.S. Department of Commerce: Washington, DC; 58.
Pederson N, Jacoby GC, D'Arrigo RD, Cook ER, Buckley BM, Dugarjav C, Mijiddorj R. 2001. Hydrometeorological reconstructions for northeastern Mongolia derived from tree rings: AD 1651–1995. *Journal of Climate* **14**: 872–881.
Stahle DW, Cleaveland MK, Hehr JG. 1985. A 450-year drought reconstruction for Arkansas, United States. *Nature* **316**: 530–532.
Trenberth KE, Overpeck JT, Solomon S. 2004. Exploring drought and its implications for the future. *Eos, Transactions-American Geophysical Union* **85**: 27–29.
van der Schrier G, Briffa KR, Jones PD, Osborn TJ. 2006. Summer moisture variability across Europe. *Journal of Climate* **19**: 2818–2834.
Wang Y, Zhou L. 2005. Observed trends in extreme precipitation events in China during 1961–2001 and the associated changes in large-scale circulation. *Geophysical Research Letters* **32**: L09707, Doi: 10.1029/2005GL022574.
Wells N, Goddard S. 2004. A self-calibrating Palmer drought severity index. *Journal of Climate* **17**: 2335–2351.
Wigley T, Briffa KR, Jones PD. 1984. On the average value of correlated time series, with applications in dendroclimatology and hydrometeorology. *Journal of Climate and Applied Meteorology* **23**: 201–213.
Wu SH, Yin YH, Zheng D, Yang QY. 2006. Moisture conditions and climate trends in China during the period 1971–2000. *International Journal of Climatology* **26**: 193–206.
Zhang R, Sumi A, Kimoto M. 1999. A diagnostic study of the impact of El Nino on the precipitation in China. *Advances in Atmospheric Sciences* **16**: 229–241.
Zou XK, Zhai PM, Zhang Q. 2005. Variations in droughts over China: 1951–2003. *Geophysical Research Letters* **32**: L04707, Doi: 10.1029/2004GL021853.